

Short-term adaptation of postprandial lipoprotein secretion and intestinal gene expression to a high-fat diet

Sandra Jimena Hernández Vallejo,^{1,2,3*} Malik Alqub,^{1,2,3*} Serge Luquet,⁵ Céline Cruciani-Guglielmacci,⁵ Philippe Delerive,⁴ Jean-Marc Lobaccaro,⁶ Athina-Despina Kalopissis,^{1,2,3} Jean Chambaz,^{1,2,3} Monique Rousset,^{1,2,3} and Jean-Marc Lacorte^{1,2,3}

¹Université Pierre et Marie Curie-Paris 6, UMR S 872, Les Cordeliers, Paris; ²INSERM, U 872, Paris; ³Université Paris Descartes, UMR S 872, Paris; ⁴Cardiovascular and Urogenital Center of Excellence for Drug Discovery, GlaxoSmithKline, Les Ulis; ⁵Université Paris-VII, CNRS UMR 7059, Paris; and ⁶Clermont Université, UMR CNRS6247; CRNH-Auvergne, Aubière, France

Submitted 5 May 2008; accepted in final form 29 January 2009

Hernández-Vallejo SJ, Alqub M, Luquet S, Cruciani-Guglielmacci C, Delerive P, Lobaccaro J, Kalopissis A, Chambaz J, Rousset M, Lacorte J. Short-term adaptation of postprandial lipoprotein secretion and intestinal gene expression to a high-fat diet. *Am J Physiol Gastrointest Liver Physiol* 296: G782–G792, 2009. First published February 5, 2009; doi:10.1152/ajpgi.90324.2008.—Western diet is characterized by a hypercaloric and hyperlipidic intake, enriched in saturated fats, that is associated with the increased occurrence of metabolic diseases. To cope with this overload of dietary lipids, the intestine, which delivers dietary lipids to the body, has to adapt its capacity in lipid absorption and lipoprotein synthesis. We have studied the early effects of a high-fat diet (HFD) on intestinal lipid metabolism in mice. After 7 days of HFD, mice displayed normal fasting triglyceridemia but postprandial hypertriglyceridemia. HFD induced a decreased number of secreted chylomicrons with increased associated triglycerides. Secretion of larger chylomicrons was correlated with increased intestinal microsomal triglyceride transfer protein (MTP) content and activity. Seven days of HFD induced a repression of genes involved in fatty acid synthesis (FAS, ACC) and an increased expression of genes involved in lipoprotein assembly (apoB, MTP, and apoA-IV), suggesting a coordinated control of intestinal lipid metabolism to manage a high-fat loading. Of note, the mature form of the transcription factor SREBP-1c was increased and translocated to the nucleus, suggesting that it could be involved in the coordinated control of gene transcription. Activation of SREBP-1c was partly independent of LXR. Moreover, HFD induced hepatic insulin resistance whereas intestine remained insulin sensitive. Altogether, these results demonstrate that a short-term HFD is sufficient to impact intestinal lipid metabolism, which might participate in the development of dyslipidemia and metabolic diseases.

enterocyte; chylomicron; lipid metabolism; SREBP-1C

IMPORTANT CHANGES IN HUMAN nutrition have occurred these last decades in most parts of the world, among which a significant increment in caloric intake and an increase in saturated fatty acid intake (8). These changes occurred concomitantly with a rise in metabolic diseases, such as obesity, metabolic syndrome, and diabetes, that are risk factors of atherosclerosis and cardiovascular diseases. Several studies have established that the development of these pathologies is associated with prolonged postprandial hypertriglyceridemia (12, 19, 26), even in patients without fasting hypertriglyceridemia (11). Dramatic

postprandial hypertriglyceridemia is frequently associated with impaired catabolism by lipoprotein lipase (LPL) of triglyceride-rich lipoproteins (TRL) and/or uptake of the ensuing remnants by tissues mainly by the LDL receptor (31).

Little attention was paid in these studies to the role that intestine, the first organ to face nutrients, could play in these metabolic disorders. Yet dyslipidemia may result from overproduction or modifications of the postprandial TRL secreted by the intestine. TRL synthesis and secretion are complex processes. Indeed, after hydrolysis of dietary fat and emulsification, resulting fatty acids and monoglycerides are taken up by enterocytes and used for triglyceride (TG) synthesis by the successive actions of monoacylglycerol acyltransferase and diacylglycerol acyltransferase at the membrane of the smooth endoplasmic reticulum (ER). After transfer in the ER lumen, TG droplets associate with primordial lipoproteins comprising apoB48 and phospholipids, through the action of microsomal triglyceride transfer protein (MTP), to form TRL. After further processing in the secretory pathway, mature chylomicrons are secreted into the lymph (17).

Changes in intestinal lipoprotein secretion have been already reported in the context of insulin resistance or diabetes, in animal models as in humans, involving enhanced activity of intestinal MTP in association with an oversecretion of apoB48 lipoproteins (23, 27). Such studies were performed when pathologies were already established. By contrast, little is known about early changes of intestinal lipid metabolism that could occur in response to high-fat diet. These potential changes deserve to be characterized, especially when considering the short lifetime of enterocytes, with a complete renewal of the intestinal epithelium within 3–4 days in mouse or 5–6 days in humans.

For this study, which intended to analyze whether such early changes in the intestinal function of dietary lipid transfer occurred, we used a diet enriched in cholesterol and in medium-chain fatty acid-containing coconut oil (Table 1), which is largely used as frying oil and in food manufacturing to provide firmness and texture. This diet was reported to induce fasting hypertriglyceridemia, hypercholesterolemia, and lipid accumulation in macrophages in rodent models (25, 33). It is known that short-chain fatty acids (C:10 and less) are directly transported through the enterocyte to circulation and are not inte-

* S. J. Hernández Vallejo and M. Alqub contributed equally to this work.

Address for reprint requests and other correspondence: J.-M. Lacorte, Centre de Recherche des Cordeliers, 15 rue de l'École de Médecine, 75006, Paris, France (e-mail: jean-marc.lacorte@crc.jussieu.fr).

The costs of publication of this article were defrayed in part by the payment of page charges. The article must therefore be hereby marked "advertisement" in accordance with 18 U.S.C. Section 1734 solely to indicate this fact.

Table 1. Composition of experimental diets

	CD, g/100 g	HFD, g/100 g
Proteins	23.5	18.7
Fibers	4.0	3.2
Ash	5.7	4.55
Carbohydrates	49.8	39.8
Moisture	12.0	9.6
Cholesterol		0.15
Fat	5.0	24
Caloric density, kcal/g	3.38	4.52
Fatty acid composition, % of total fatty acids		
8:0		7.3
10:0		5.1
12:0		40.6
14:0		16.6
16:0	22.1	10.1
16:1	2.2	1.0
18:0	11.2	4.3
18:1	26.4	5.0
18:2	38.1	10.0

CD, chow diet; HFD, high-fat diet.

grated into chylomicrons. On the other hand, long-chain fatty acids (C:16 and longer) are used for de novo synthesis of TG, which are incorporated into chylomicrons secreted in lymph. Much less is known about medium-chain fatty acids, for which studies revealed very heterogeneous results. Indeed, for C:12 and C:14 fatty acids, both direct transport into circulation and TRL-associated secretion were reported (24). These reasons prompted us to investigate whether a short-term high-fat diet composed of coconut oil would induce a rapid adaptation of intestinal function and impact the enterocyte of TRL secretion.

We demonstrate that 7 days of HFD were sufficient to decrease plasma apoB content, to enhance postprandial triglyceridemia, and to induce adaptation of intestinal gene expression.

EXPERIMENTAL PROCEDURES

Animals and diets. Male C57BL/6 mice (6–8 wk, 20–25 g) purchased from Charles River (St. Germain l'Arbresle, France), liver X receptor (LXR)- α/β knockout mice (4) and their wild-type littermates were maintained in an environmentally controlled facility with diurnal light cycle (7 AM–7 PM) with free access to food and water for 2 wk before use. Then mice housed in individual cages received ad libitum either a chow diet (AO3; SAFE, France) or a high-fat/high-caloric diet (HFD), detailed in Table 1, for 7 days. HFD was obtained by the addition of hydrogenated coconut oil (20% wt/wt) and cholesterol (0.15% wt/wt) to the chow diet (CD). In another experiment, the LXR agonist T09013117 (8.33 mg/g body wt) or the vehicle (methylcellulose) were administered daily by oral gavage at 6 PM for 2 successive days. All experiments were performed at 12:00, i.e., 4 h after food withdrawal. During this period, animals had free access to water. All experimental procedures were in accordance with institutional regulations for the care and use of laboratory animals.

Plasma analysis. After anesthesia, blood was collected from the inferior vena cava into EDTA-containing tubes, and the plasma was isolated by low-speed centrifugation at 4°C. Cholesterol and triglycerides were measured on Olympus AU-600 Diagnostics with enzymatic kits. Insulin was measured with an ELISA kit from Linco Research (St. Charles, MO). Blood glucose was determined in samples taken from the tail vein, by using Glucotrend glucometer and Accu-Chek strips (Roche Diagnostics, Meylan, France).

MTP activity assay. Intestinal epithelium was scrapped and sonicated in homogenization buffer containing 10 mM Tris·HCl (pH 7.4),

150 mM NaCl, 1 mM EDTA, and 2% protease inhibitor cocktail (Sigma-Aldrich). MTP activity was measured with an MTP assay kit (Roar Biomedical, New York, NY) by incubating, for different times at 37°C, 100 μ g of proteins of intestinal epithelium homogenates with 4 μ l of donor solution and 4 μ l of acceptor solution (according to manufacturer's instructions) in homogenization buffer (total volume 200 μ l). Fluorescence was measured (485-nm excitation wavelength and 538-nm emission wavelength) at 37°C every 15 min for 115 min using the Fluostar Ascent FL (Labsystems, Paris, France).

Preparation of microsomes. The first third of the small intestine from five mice was excised (7–10 cm length), flushed with 10 ml of washing buffer (117 mM NaCl, 5.4 mM KCl, 2.6 mM NaHCO₃, 5 mM HEPES, 5.5 mM glucose, 0.96 mM NaH₂PO₄) via a syringe-attached catheter. Intestine was then everted and cut into 3-mm pieces that were then incubated with Matrisperse (BD Biosciences) at 4°C overnight. The intestinal epithelium was filtered and washed with PBS. The filtrate was homogenized in 0.25 M sucrose, 10 mM Tris-Cl, pH 7.5, 3 mM MgCl₂ and 2% protease inhibitor cocktail by 10 strokes up and down, 800 rpm at 4°C in a glass Potter homogenizer. The homogenate was centrifuged (300 g for 5 min at 2°C). The supernatant was then centrifuged (100,000 g for 1 h at 4°C) to obtain microsomes.

Extraction of nuclear proteins. The filtered epithelium (as described above) was homogenized with *buffer A* (0.02 M HEPES pH 7.9, 1.5 mM MgCl₂, 0.01 KCl, 0.05 M NaF, 2 mM orthovanadate, 0.5 mM DTT, 0.5 mM spermidine, 0.15 mM spermine, 5 μ g/ml leupeptin, and 2% protease inhibitors), vortexed, and incubated at 4°C for 10 min and then centrifuged (3,000 rpm for 10 min at 4°C). The supernatant was removed and the pellet was homogenized with *buffer B* (0.02 M HEPES pH 7.9, 1.5 mM MgCl₂, 0.05 M NaF, 0.5 M NaCl, 2 mM orthovanadate, 0.5 mM spermidine, 0.15 mM spermine, 0.5 mM EDTA, 25% glycerol, 5 μ g/ml leupeptin, and 2% protease inhibitor cocktail) and centrifuged at 13,000 rpm for 30 min at 4°C; the supernatant containing nuclear proteins was recovered and stored at –80°C.

Western blot analysis. The first third of the small intestine was excised (7–10 cm length), flushed with 10 ml of washing buffer. Intestine was then everted, rinsed with cold PBS, and scraped with a glass slide. The scraped tissue was homogenized by sonication in 1 ml lysis buffer containing 5% protease inhibitor cocktail (Sigma-Aldrich), 1% Triton X-100, 5 mM EDTA, and PBS.

Forty micrograms of total proteins or 2 μ l of plasma (containing protease inhibitor cocktail) were loaded on 5% SDS-PAGE gels for apoB and E-cadherin detection or 12% SDS-PAGE gels for MTP and α -actin detection. For apoB, blots were probed by using goat polyclonal anti-human apoB antibody (1/10,000) (Chemicon) and then peroxidase-conjugated horse anti-goat IgG (1/10,000) (Vector Laboratories, AbCys). For MTP, blots were probed with a mouse monoclonal anti-mouse MTP antibody (BD Biosciences, 1/2,500) and then peroxidase-conjugated sheep anti-mouse IgG antibody (1/10,000) (Amersham). ApoB and MTP levels were normalized by α -actin or E-cadherin expression by use of mouse anti-actin monoclonal antibody (Chemicon, 1/2,000) or mouse anti-E-cadherin monoclonal antibody (Takara Bio, 1/2,500), respectively. For sterol regulatory element binding protein (SREBP)-1c, 80 μ g of microsomal fractions and 60 μ g of nuclear extracts were subjected to 12% SDS-PAGE and probed by use of mouse monoclonal anti-mouse SREBP-1c antibody. The mature form of SREBP-1c in nuclear extracts was normalized by C/EBP α expression (antibody anti-C/EBP α from Santa Cruz). The blots were developed with ECL Western blotting reagents according to the manufacturer's instructions (Amersham). Films were scanned and quantified by using Image-Quant software (Molecular Dynamics).

Analysis of postprandial lipoprotein secretion. After 4 h of fasting, between 8:00 and 12:00 AM mice fed CD or HFD received 150 μ l of coconut oil bolus by gavage. For each feeding condition, five mice were killed before the lipid bolus, to determine baseline parameters

(time 0), and at the indicated times after bolus (30, 60, 90, 180, and 270 min).

To determine lipoprotein secretion, mice received an intraperitoneal injection of 1 μg Tyloxapol WR-1339 (Sigma-Aldrich) per gram of body weight and 30 min later mice were force fed with 150 μl of coconut oil containing [$1\text{-}^{14}\text{C}$]oleic acid (2 μCi , specific activity 50 $\mu\text{Ci}/\mu\text{mol}$, 8.17% of total fat of the bolus) (PerkinElmer). Two hours after Triton injection, animals were euthanized. EDTA plasma from 10 mice per group were pooled. Chylomicrons were prepared by ultracentrifugation at 10,000 g for 30 min at 20°C. A second ultracentrifugation was performed at 100,000 g for 18 h at 10°C to isolate VLDL. Lipids were extracted from each fraction and separated by TLC as previously described (39). After autoradiography, radioactive spots corresponding to TG were excised and counted in a scintillation counter (Beckman).

RNA extraction and semiquantification by real-time RT-PCR. Total RNA was extracted from liver and scraped mucosa of small intestine by using Tri Reagent (Euromedex) according to the manufacturer's instructions. cDNA was synthesized from 1 μg of total RNA in 20 μl , by using random hexamers and murine Moloney leukemia virus reverse transcriptase (Invitrogen, Cergy Pontoise, France) as recommended by the manufacturer. Primers for apoA-IV, apoB, apoC-III, FAS, ACC, MTP, SCD1, SREBP-1c, SREBP-2, liver X receptor (LXR)- α , hepatocyte nuclear factor 4 (HNF4)- α , peroxisome proliferator-activated receptor (PPAR)- γ 2, PPAR α , and ABCA1 genes (Table 2) were obtained from MWG-Biotech (Paris, France). Semiquantitative RT-PCR analyses were performed with 50 ng of reverse-transcribed total RNA in 1 \times LC FastStar DNA Master Plus SYBRgreen I buffer (Roche Diagnostics, Meylan, France), and 200 nM of each sense and antisense primer in a final volume of 10 μl using the LightCycler apparatus (Roche Diagnostics). Expression of 18S rRNA was quantified by using Predeveloped Taqman Assay Reagent (Applied Biosystems, Les Ulis, France) and LC FastStart DNA Master Plus Hybridization probes (Roche Diagnostics) as recommended by the manufacturers. Total RNA from mice fed CD was used to obtain standard curves. In summary, cDNA of mice fed CD was subjected to serial dilutions, amplified along with samples, and plotted in arbitrary units to acquire quantitative data with the LightCycler software. Expression data for mRNA levels were normalized compared with 18S rRNA and expressed in arbitrary units. All samples were assayed in duplicate, and the average value of the duplicates was used for relative quantification.

Hyperinsulinemic-euglycemic clamp studies. Mice were catheterized at least 6 days before the experiment after being anesthetized with a mixture of ketamine and xylazine (100 and 10 mg/kg body wt, respectively).

The right jugular vein was catheterized for infusion with a Silastic catheter (0.025 OD). The free end of the catheter was tunneled under

the skin to the back of the neck and passed through a piece of Tygon tubing, glued together, and secured to the skin. Catheters were flushed daily with ~ 50 μl of 0.9% NaCl containing 5 mg/ml ampicillin and 20 IU/ml heparin.

Animals were individually housed after surgery and their body weight was monitored daily. Animals were excluded from the study at day 6 postsurgery if weight loss was greater than 10% of presurgery weight. After being fasted for 6 h, awake animals were placed unrestrained in their home cage for the duration of the clamp experiment. After a bolus infusion of 5 μCi of D-[3- ^3H]glucose (Amersham Biosciences) tracer solution and 80 mU/kg insulin (1), the tracer was infused continuously (0.025 $\mu\text{Ci}/\text{min}$, at a constant rate of 5 $\mu\text{l}/\text{min}$) for the duration of the experiment and insulin infusion was kept constant at 0.2 IU $\cdot\text{kg}^{-1}\cdot\text{h}^{-1}$ (3.33 mU $\cdot\text{kg}^{-1}\cdot\text{min}^{-1}$). Blood glucose levels were determined from tail blood samples (5 μl) at $t = 0$ and then every 15 min (glucose analyzer Accu-check, Roche). Steady state was ascertained when glucose measurements were constant for at least 20 min at a fixed glucose infusion rate, and this was achieved within 50 to 80 min. At steady state, two blood samples (25 μl) were collected for determination of basal parameters, followed by a bolus injection of 2-deoxy-D-[1- ^{14}C]glucose (2DG) (5 μCi , Amersham). Blood samples (20 μl) were collected from the tail at 0, 5, 10, 20, 30, 40, 50, and 60 min until the end of the experiment, when mice were killed by pentobarbital injection and tissues were collected. Basal and steady-state plasma [3- ^3H]glucose radioactivity was measured as described (21). Tissue glucose turnover rate (mg $\cdot\text{kg}^{-1}\cdot\text{min}^{-1}$) was calculated as described (21). In vivo glucose uptake (ng $\cdot\text{mg}^{-1}\cdot\text{min}^{-1}$) for muscle (tibialis anterior, soleus, extensor digitorum longus), white adipose tissue (subcutaneous, periepididymal, visceral), intestinal muscle and intestinal epithelium was calculated on the basis of the accumulation of 2DG-6-phosphate in the respective tissue and the disappearance rate of 2DG from plasma as described (21).

For [3- ^3H]glucose determination, plasma was deproteinized with Ba(OH) $_2$ and ZnSO $_4$. For each sample, an aliquot of the supernatant was counted directly and another was dried to remove $^3\text{H}_2\text{O}$. Plasma $^3\text{H}_2\text{O}$ was determined as a difference between dried and undried samples. Immunoreactive insulin was determined as described (21).

Glucose rates of appearance (R_a) and disappearance (R_d) were determined by using Steel's non-steady-state equation. Endogenous glucose production (Endo R_a , given as mg $\cdot\text{kg}^{-1}\cdot\text{min}^{-1}$) was determined by subtracting the glucose infusion rate from total R_a . Glycolytic rates were estimated from the increment per unit of time of $^3\text{H}_2\text{O}$ multiplied by the estimated body water divided by [3- ^3H]glucose specific activity. $^3\text{H}_2\text{O}$ appearance was determined by linear regression of the measurement at $t = 80$ to $t = 120$ min. Body water was assumed as 60% of body weight.

Table 2. Sequence of primers for semiquantitative RT-PCR

Gene	mRNA Transcript Size	Primer Sense 5'→3'	Primer Antisense 5'→3'
apoA-IV	379	GGATTACTTTACCCAGCTAAGCA	GGTCAGCTGGAGCTTCATT
apoB	223	AGTGCGTGCAGTGGATCAAGTACCTGC	TGGACAGCTGAAGCTTAAGTTTCCAGGAC
apoC-III	297	CTACTCCAGGTACGTAGGTGCC	TGGTCCTCAGGGTTAGAATCCC
FAS	116	TCAACCGTAAGCCCTTGTTT	CTCAGCAACCCGGACATC
ACC	102	GCCATTGGTATTGGGGCTTAC	CCCGACCAAGGACTTTTGTTG
MTP	64	GCTCCGTCAGCTGGTGGAT	CAGGATGGCTTCTAGCGAGTCT
SCD1	62	TTCCCTCCTGCAAGCTCTAC	CAGAGCGCTGGTCATGTAGT
SREBP-1c	116	ATCGGGCGGAAGCTGTCGGGGTAGCGTC	ACTGTCTGGTTGTTGATGAGCTGGAGCAT
SREBP-2	204	CCCTTGACTTCCTTGCTGCA	GCGTGAGTGTGGCGCAATC
LXR α	85	CTGCAGCCCTACGTCTCCAT	AAGTACGGAGGCTCACCAGCTT
HNF4 α	218	GGTCTGCCAGTGATGCAC	CAGGAGCTTGTAGGATTCAG
PPAR γ 2	71	TGACAGGAAAGACAACGGACAA	ATCTTCTCCCATCATTAAAGGAATTCAT
PPAR α	101	GCAGTGCCCTGAACATCGA	TGC CGAAGAAAGCCCTTA
ABCA1	102	CCCAGAGCAAAAAGCGACTC	GGTCATCATCACTTTGGTCCTTG

Statistical analysis. Results are given as means \pm SE. Statistical analysis was performed with Excel software (Microsoft), and differences were determined with the *t*-test for nonpaired samples.

RESULTS

Effects of a short-term HFD on body weight and plasma parameters. C57Bl/6 mice were fed, for 7 days, either a CD with lipids accounting for 13% of total energy or HFD with lipids accounting for 48% of total energy and 0.15% (wt/wt) cholesterol. As shown in Fig. 1A, weight gain over 7 days was similar with both diets. In the HFD group, fasting plasma total cholesterol and nonesterified fatty acids were increased (Fig. 1, C and F), without significant change in fasting triglyceridemia (Fig. 1B). In addition, glycemia and insulinemia were also increased, indicating that a short-term HFD might have a

possible effect on insulin sensitivity (Fig. 1, D and E). Moreover, analysis of lipoprotein profile of fasting mice plasma showed that the increase in plasma cholesterol was correlated with increased in HDL-cholesterol (data not shown). Since mice do not naturally express cholesteryl ester transfer protein, the normal fasting TG level and the increase of HDL are consistent with an adequate LPL activity, as was previously described (37).

Short-term HFD induces changes in postprandial TRL. To characterize the postprandial kinetics of TRL after a short-term HFD, mice were fasted for 4 h and then received an oral lipid bolus of coconut oil. In mice fed CD, triglyceridemia increased moderately 30 min after the oral lipid load and decreased rapidly thereafter (Fig. 2A). This modest peak of TG, which differs from the elevated peak occurring 3 h after the oral load

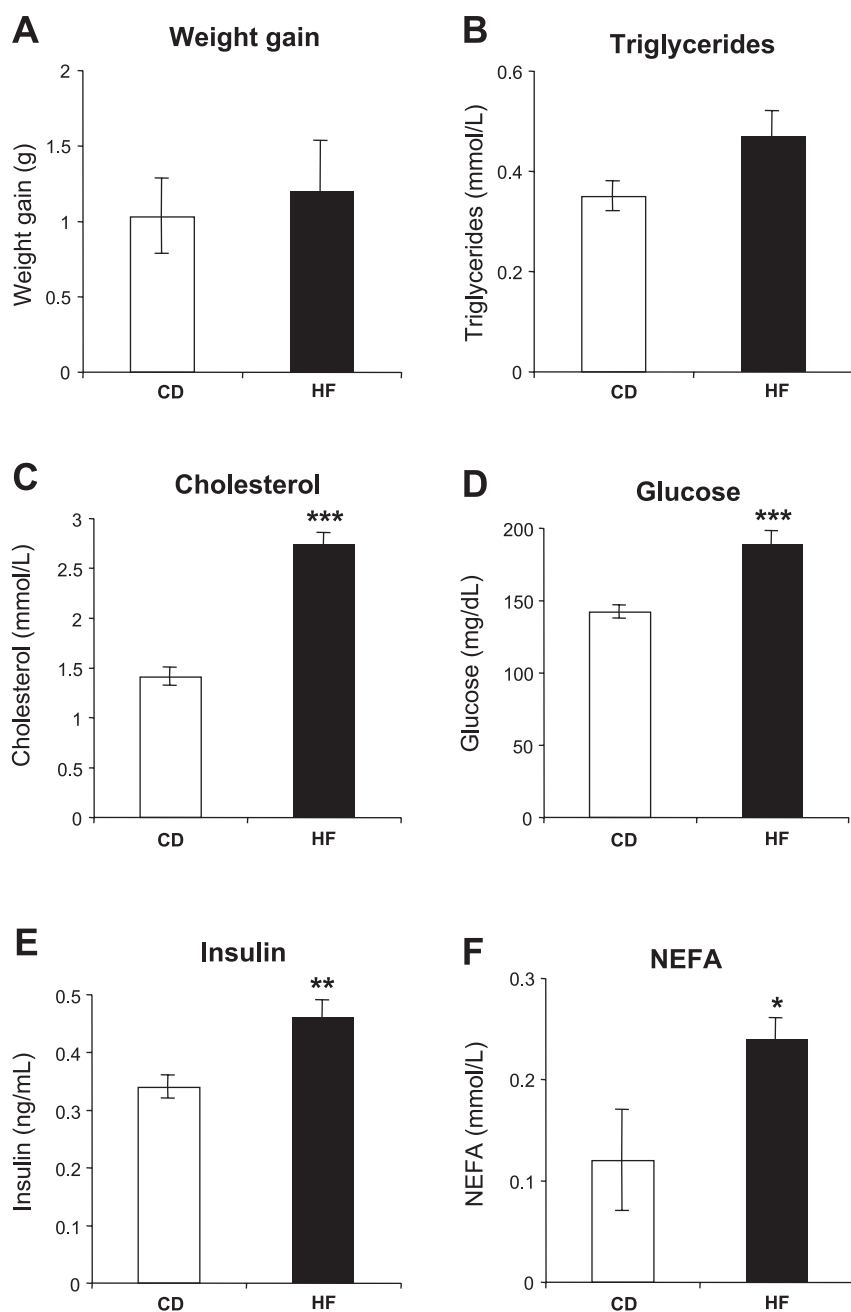
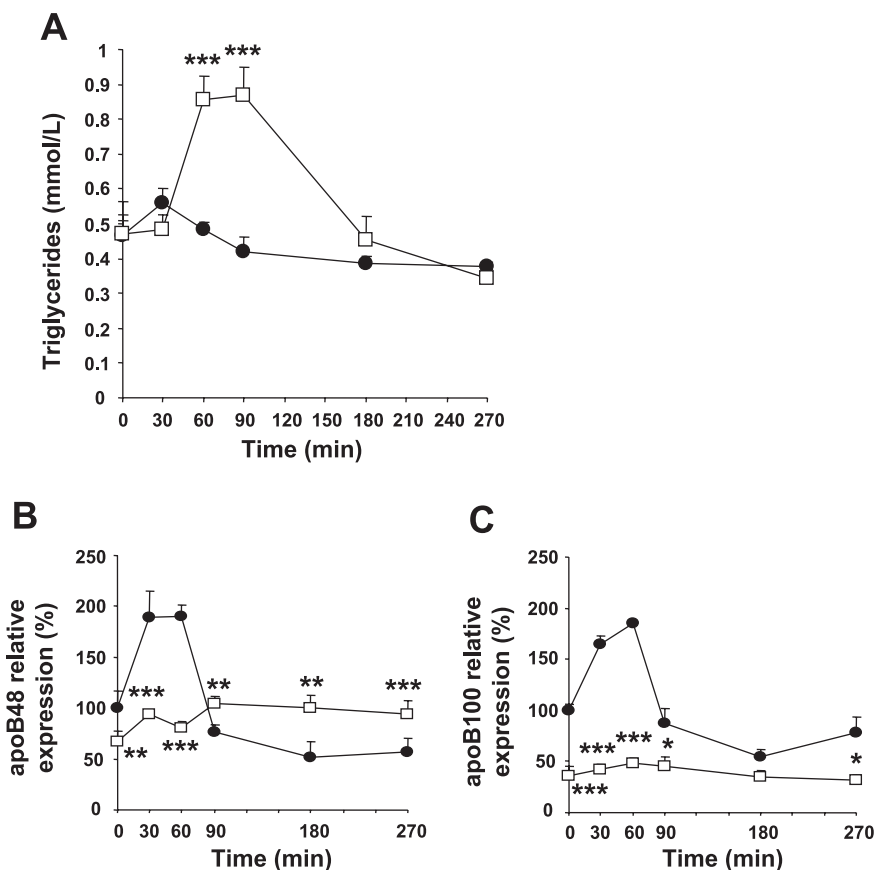


Fig. 1. Body weight and plasma parameters during short-term, high-fat (HF) diet (HFD). Individually housed mice, were fed either a chow diet (CD) or a HFD during 7 days. Body weight was measured every day. Weight gain (A) represents the difference between the initial weight and the weight at the end of the regimens. Plasma triglycerides (B), cholesterol (C), glucose (D), insulin (E), and nonesterified fatty acids (NEFA; F) were measured at 12:00, after 4 h of fasting. Data are means \pm SE obtained from 15–20 mice. * P < 0.05, ** P < 0.01, *** P < 0.001 HFD vs. CD.

Fig. 2. Effects of HFD on postprandial triglycerides and apoB isoforms. Mice were fed CD or HFD for 7 days. At 4 h after food withdrawal, mice received an oral lipid load of 150 μ l of coconut oil. Blood was collected from the abdominal vein at 0, 30, 60, 90, 180, and 270 min after the lipid bolus. **A**: plasma triglyceride levels were measured in mice fed CD or HFD for 7 days. Relative apoB48 and apoB100 expressions were determined by Western blot followed by densitometric scanning of the specific band. Values are expressed as the percentage of apoB48 (**B**) or apoB100 (**C**), the amounts obtained in CD mice at *time 0* being set at 100%. ●, Mice fed CD; □, mice fed HFD for 7 days; $n = 5-8$ for each time point. * $P < 0.05$; ** $P < 0.01$; *** $P < 0.001$ vs. CD.



of long-chain fatty acids (6), may be due to the use of coconut oil, composed of ~60% of medium-chain fatty acids that are in part directly delivered to the portal vein and in part incorporated into chylomicron-associated TG (24). CD animals also exhibit an early increased in apoB-100 protein, which has an exclusive hepatic origin, coincident with an increased apoB48 (Fig. 2, *B* and *C*). These results suggest that, in mice fed CD, liver has the capability to secrete apoB-100-containing particles relatively early by using the fatty acids delivered in portal vein. Seven days of coconut oil HFD resulted in dramatic changes of postprandial triglyceridemia, without affecting fasting TG levels (Fig. 1). Plasma TG peaked between 60 to 90 min and the peak was 1.6-fold higher than in CD-fed mice (Fig. 2A), suggesting that, after a short-term HFD, enterocytes and/or hepatocytes may become able to efficiently use medium-chain fatty acid for TG synthesis. Nevertheless, after 7 days of HFD, the increase of triglycerides occurred within 60 min after lipid bolus, a too short time lapse for the digestion of TG from bolus, the intestinal absorption of resulting fatty acids and monoglycerides, the liver uptake of fatty acids, the synthesis of triglycerides, and the secretion of corresponding VLDL. Moreover, apoB-100 levels in HFD mice at 60 min and 90 min after the bolus were not significantly different from basal apoB-100 at 0 min (Fig. 2C), arguing in favor of an intestinal origin of the observed TG peak.

At the same time, fasting and postprandial apoB48 and apoB100 were assessed in CD or HFD fed mice. In CD mice, apoB48 peaked between 30 and 60 min after the lipid bolus, then decreasing below the fasting levels between 90 and 270 min (Fig. 2B). Interestingly, HFD mice displayed lower fasting

apoB48 levels compared with CD (Fig. 2B, *time 0*) and dramatically different kinetics after the bolus: a small increase at 30 and 60 min, and sustained levels of corresponding apoB48 between 90 and 270 min, which are higher than CD mice. At the same time, fasting apoB100 was considerably lower in HFD mice than in CD mice, with the virtual absence of an early peak at 30 and 60 min (Fig. 2C). These results suggest that elevated postprandial triglyceridemia after 7 days of HFD is likely associated with apoB48-containing TRL rather than apoB100-containing TRL.

Short-term HFD induces increased intestinal synthesis of triglycerides and decreased number of secreted chylomicrons. To measure TRL secretion, mice were injected with Triton WR-1339, which inhibits lipoprotein lipase activity and thus TRL catabolism. In addition, mice were force fed with a bolus of coconut oil. To avoid bias due to the direct transfer of medium-chain fatty acid to portal vein and to strictly quantify intestinal TG synthesis, long-chain [$1-^{14}$ C]oleic acid was used as a radiolabeled tracer. This does not preclude that differential incorporation of the two types of fatty acid into the particle during assembly and differential removal during catabolism in the two dietary groups may occur. Ninety minutes after bolus, postprandial TRL were isolated by sequential ultracentrifugation to separate chylomicrons of intestinal origin and VLDL of both hepatic and intestinal origins.

The apoB48 content of the chylomicron fraction was lower in HFD compared with CD mice whereas newly synthesized [$1-^{14}$ C]TG and total TG were greatly increased (Fig. 3, A–C). By contrast, there was no significant change in the amounts of apoB48 and newly synthesized [$1-^{14}$ C]TG in the VLDL frac-

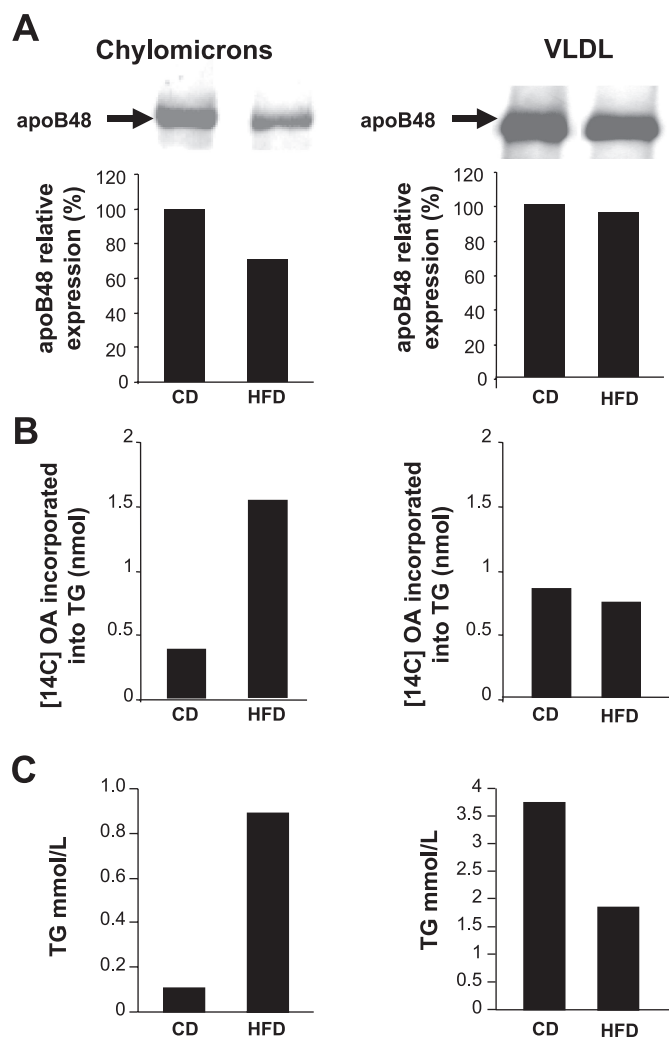


Fig. 3. Effects of HFD on apoB isoforms, total triglyceride (TG), and $[1-^{14}\text{C}]$ triglyceride of chylomicrons and VLDL. Mice were fed CD or HFD for 7 days. At 3 h 30 min after food withdrawal, mice received an intraperitoneal injection of Triton WR-1339 ($1 \mu\text{g}/\text{g}$ body wt) and 30 min later received a bolus of coconut oil ($150 \mu\text{l}$) containing $[1-^{14}\text{C}]$ oleic acid (OA). Ninety minutes later, blood was collected from the abdominal vein. Plasma from 10 mice was pooled and lipoproteins were separated by sequential ultracentrifugation. **A**: apoB48 in chylomicrons and VLDL was analyzed by Western blot and quantified by densitometric scanning. The level of apoB48 in CD fed mice was set at 100%. **B**: lipids were extracted from chylomicrons and VLDL and, after separation by TLC, $[1-^{14}\text{C}]$ triglyceride was counted. **C**: total triglyceride levels were measured in chylomicrons and VLDL.

tion, whereas the total VLDL-TG content was even decreased after 7 days of HFD (Fig. 3C). This decrease in total VLDL-TG could be related to an impairment of the secretion of hepatic VLDL paralleling that of apoB100 (Fig. 2C). Therefore, we might suggest that the maintenance of apoB48-containing VLDL levels could be due to an increase in intestinal VLDL secretion. Because in mice apoB48 is produced by both intestine and liver, it is not possible to distinguish in plasma the proportions of apoB48-containing VLDL originating from liver or intestine.

Whatever the case, our results showed changes in the distribution of postprandial TRL between chylomicrons and VLDL under a short-term HFD. By contrast, Western blot analysis revealed no difference in the amounts of apoB48 in the

intestinal mucosa after 7 days of HFD compared with CD (0.98 ± 0.08 vs. 0.87 ± 0.05 au, respectively; $P = 0.28$). Therefore, these results suggest that the early intestinal response to a lipid overload consisted of an increased TG synthesis, a decreased secretion of chylomicrons overloaded with TG, and a maintained or increased secretion of apoB48-containing TRL in the density range of VLDL.

Short-term HFD increases MTP amount and activity. We then analyzed whether the 7 days of HFD induced an augmentation of MTP activity that would be consistent with increased chylomicron lipidation. Results obtained with microsomal fractions of the intestinal mucosa showed that both MTP amount (Fig. 4A) and activity (Fig. 4B) were increased in mice fed HFD compared with CD.

Short-term HFD induces hepatic but not intestinal resistance to insulin. As shown in Fig. 1, HFD induced fasting hyperinsulinemia that might reveal insulin resistance. However, this result could not explain easily the effects on intestinal lipid metabolism. Indeed, it has been recently reported that a bolus of insulin decreased plasma apoB48 (7), whereas increased intestinal MTP mass and activity have been correlated with insulin deficiency or insulin resistance (10, 34). To evaluate the consequences of the short-term HFD on insulin sensitivity, we performed hyperinsulinemic-euglycemic clamp analysis. In this experiment, the determination of glucose infusion rate (GIR) required to maintain euglycemia, when insulin is maintained high ($0.2 \text{ IU}\cdot\text{kg}^{-1}\cdot\text{min}^{-1}$), allows the determination of EndoR_a by subtracting the GIR from the R_a . Under hyperinsulinemia, endogenous glucose production, measured at steady state, reflects insulin's ability to suppress hepatic glucose production. As shown in Fig. 5, a short-term HFD is sufficient to induce hepatic insulin resistance, since EndoR_a was higher in mice fed HFD compared with mice fed CD (18.84 ± 1.15 vs. $14.45 \pm 0.85 \text{ mg}\cdot\text{kg}^{-1}\cdot\text{min}^{-1}$, $P = 0.02$). However, whole body glucose uptake was similar in both groups (29.36 ± 0.99 vs. $26.79 \pm 0.49 \text{ mg}\cdot\text{kg}^{-1}\cdot\text{min}^{-1}$, not significant), and the insulin-stimulated glucose uptake rates in skeletal muscle, adipose tissue, intestinal epithelium, and

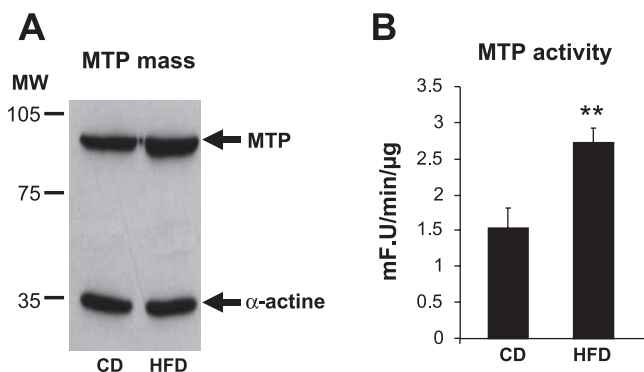


Fig. 4. Short-term HFD increases microsomal triglyceride transfer protein (MTP) amount and activity. **A**: $40 \mu\text{g}$ of intestinal microsomal proteins, prepared from mice fed HFD or CD for 7 days, were separated by SDS-PAGE and immunoblotted with antibody against MTP and α -actin. Representative Western blot (from 3 independent experiments) shows increased MTP mass in microsomal fraction. **B**: MTP activity in intestinal epithelium homogenates of mice fed HFD or CD for 7 days. Results are expressed as fluorescence (F) units $\cdot \text{min}^{-1} \cdot \mu\text{g}$ of protein $^{-1}$; $n = 5$ mice for each condition. ** $P < 0.01$. MW, molecular weight expressed as kDa.

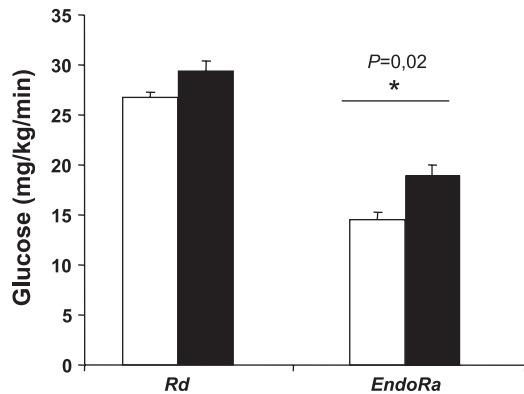


Fig. 5. Effect of a short-term HFD on glucose metabolism as assessed by hyperinsulinemic -euglycemic clamp analysis. Hepatic glucose production ($EndoR_a$) and glucose rate of disappearance (R_d) were determined during hyperinsulinemic-euglycemic clamp on unrestrained awake mice fed CD (open bars, $n = 5$) or HFD (solid bars, $n = 5$) for 7 days. * $P < 0.05$ vs. CD.

intestinal muscle were also similar between CD-fed and HFD-fed mice (data not shown).

Adaptation of intestinal gene expression under HFD. Changes in intestinal lipid metabolism might be associated with a

coordinated control of gene expression. We therefore quantified the expression of genes involved in lipid and lipoprotein synthesis and secretion. As shown in Fig. 6A, HFD induced an increase in the expression of apoA-IV, apoB, and MTP genes and a decrease in the expression of apoC-III, FAS, and ACC genes in intestine. This pattern suggested that the short-term intestinal adaptation to HFD led to the inhibition of de novo fatty acid synthesis, as expected, and to the stimulation of lipoprotein assembly and secretion. In parallel, we quantified the expression of lipid-sensor or lipid-dependent transcription factor genes. We noted a dramatic increase in the expression of SREBP-1c in the intestine of HFD compared with CD mice. In addition, short-term HFD moderately raised LXR α expression in the intestine and had no effect on SREBP-2, HNF4 α , PPAR γ 2, and PPAR α . Besides, with the exception of FAS mRNA, no significant change was observed in the expression of these genes in liver (Fig. 6B), stressing that liver and intestine respond differently to a short-term HFD.

HFD induces an increased amount of SREBP1-c and its translocation to the nucleus. To address the question of whether the increased level of intestinal SREBP-1c mRNA was physiologically relevant, the quantification of SREBP-1c protein was performed in microsomal preparations and in nuclear

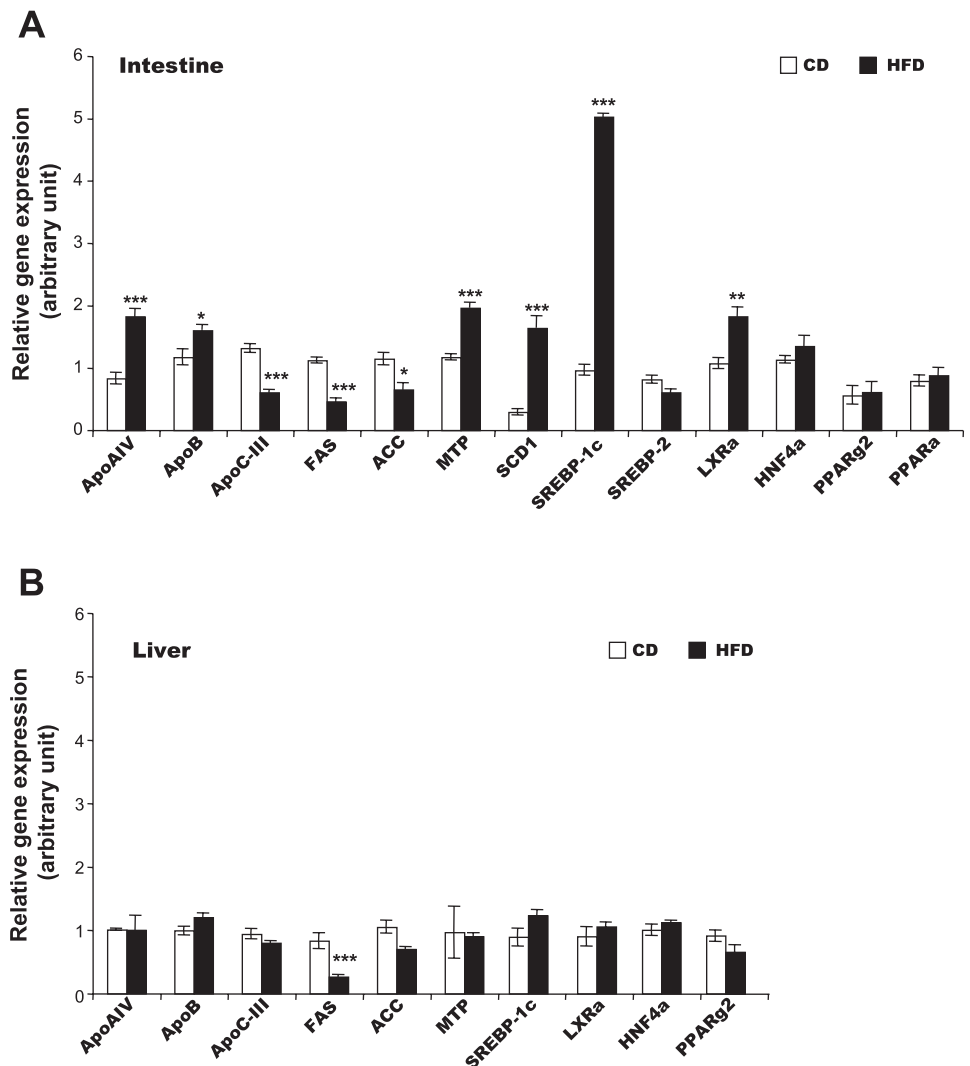


Fig. 6. Relative quantitative RT-PCR analysis of gene expression in intestine and liver after 7 days HFD. Relative gene expression in intestine (A) and liver (B) was quantified by real-time PCR. Values were normalized to the 18S rRNA and expressed as arbitrary units. Values shown are means \pm SE ($n = 8-15$). * $P < 0.05$, ** $P < 0.01$, *** $P < 0.001$ HFD (solid bars) vs. CD (open bars).

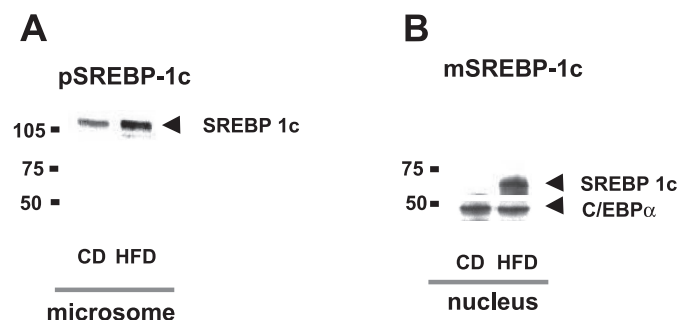


Fig. 7. Short-term HFD increases precursor and mature forms of sterol regulatory element binding protein (SREBP)-1c in intestine. *A*: after preparation of microsomal fractions from intestinal mucosa of mice fed HFD or CD for 7 days, 80 μ g of microsomal proteins were separated by SDS-PAGE and immunoblotted with antibody against SREBP-1c. Representative Western blot (from 3 independent experiments) shows precursor form of SREBP-1c (pSREBP-1c) in microsomal fraction. *B*: representative Western blot (from 2 independent experiments) shows levels of mature form of SREBP-1c (mSREBP-1c) in the nuclear extracts prepared from intestinal mucosa of mice fed HFD or CD for 7 days.

extracts of intestine. As shown in Fig. 7, the amount of the precursor form of SREBP-1c (pSREBP-1c) in microsomes and that of the mature form (mSREBP-1c) in nuclear extracts were increased in HFD-fed compared with CD-fed mice. These results demonstrated that short-term HFD activated SREBP-1c by increasing its synthesis, cleavage, and translocation to the nucleus in intestinal cells.

Intestinal activation of SREBP-1c during short-term HFD is in part independent of LXR. It has been established that insulin may activate SREBP-1c. Because the mRNA level of LXR α increased after 7 days of HFD, we hypothesized that LXR may also be involved in the HFD-induced greater expression of SREBP-1c, a target gene of LXR. After an oral gavage with T0901317, an LXR agonist, the expression of LXR-target genes was analyzed in liver and intestine. As expected, two gavages with LXR activator induced an increase in SREBP-1c, ABCA1, and FAS mRNA in liver (Fig. 8A). At the same time, we noted an increase in SREBP-1c and ABCA1 mRNA in intestine (Fig. 8B). Unexpectedly, the intestinal FAS mRNA level sharply decreased, as already observed after 7 days of HFD, suggesting that LXR was involved directly or indirectly in the control of FAS mRNA level in intestine. To test the role of LXR in the HFD-induced transcriptional activation of SREBP-1c in intestine, we fed LXR-deficient mice with HFD. HFD induced an increase in intestinal SREBP-1c, apoA-IV, and MTP expression and a decrease in FAS mRNA, irrespective of whether LXR α and LXR β were expressed or not (Fig. 8C). Because SREBP-1c activation by HFD persisted in LXR-deficient mice, our results suggest that the transcriptional activation of SREBP-1c during short-term HFD was not entirely dependent on LXR.

DISCUSSION

It is commonly admitted that high-fat diets administered over several weeks induce features of metabolic syndrome, e.g., hypertriglyceridemia, hypercholesterolemia, and hyperglycemia, and increase the risk of developing diabetes and obesity. Several studies in human and animal models demonstrated that a long-term administration of coconut diet, which is enriched in medium-chain saturated fatty acids, with or without

cholesterol addition, increased fasting triglyceridemia and cholesterolemia (15, 20, 36). Our study focused on the first steps of intestinal adaptation and postprandial response to HFD before establishment of pathologies.

We report for the first time that, during a short-term HFD, intestine adapts its postprandial secretion of TRL by decreasing the number of apoB48-containing particles in the chylomicron fraction and by increasing triglyceride synthesis and secretion. Since it is known that there is one molecule of apoB48 per chylomicron (29), this adaptation led to the secretion of a smaller number of larger-sized chylomicrons. Moreover, an increased intestinal MTP content and activity correlated with the increased lipidation of chylomicrons. These results are interesting in the light of studies in rodents and humans reporting an increased postprandial intestinal lipoprotein secretion through the increased synthesis and secretion of both triglycerides and apoB48 after a long-term HFD containing long-chain fatty acids (3, 18, 40). To our knowledge, only one report described the effects of coconut oil on postprandial lipid metabolism and showed a greater increase in triglyceride response in rabbits fed a long-term coconut oil-containing regimen than in rabbits fed olive oil (38). However, in this report, regimens were administered for 4 wk. Therefore our results obtained after a short-term HFD suggest that intestinal adaptation to HFD has at least two phases: the first phase, which may be considered as an emergency step, is to increase the size of postprandial TRL to manage lipid overloading. This early adaptive response of intestine may also facilitate TRL catabolism since it is known that the activity of LPL, the enzyme responsible for the first and rate-limiting step of TRL-TG hydrolysis, depends on physicochemical characteristics of TRL, such as particle size and composition (2, 30, 41), large chylomicrons being more rapidly catabolized than smaller ones. A second phase of intestinal adaptation appears upon longer term maintenance of dietary lipid loading when intestine probably amplify lipid delivery efficiency by increasing numbers of postprandial apoB48-TRL as usually reported. However, we cannot exclude that the early changes we report in postprandial lipoproteins might be a specific effect of coconut oil on intestinal lipoprotein secretion or clearance. Further studies using different dietary fatty acids should be performed to address the question of whether these changes in postprandial lipoproteins are a more general phenomenon.

We observed that the early adaptation of intestine to HFD was associated with coordinated changes in the expression of genes involved in lipid metabolism, e.g., a markedly decreased expression of genes involved in fatty acid synthesis (FAS and ACC), and an increased expression of genes involved in TG transport and delivery (apoB and MTP) and/or signaling (apoA-IV). Several transcription factors have been described as modulators of lipid metabolism, among which the members of nuclear receptor family HNF4, PPAR $\alpha/\delta/\gamma$, LXR α/β , farnesyl X receptor (FXR), and SREBP-1/2. We show that, after 7 days of HFD, the mature form of SREBP-1c is increased and translocated to the nucleus where it might be transcriptionally active, as suggested by the increase of SCD1 expression, one of its target genes. However, activation of SREBP-1c is not sufficient to explain all of the observed transcriptional changes in intestinal cells during HFD, such as the decreased FAS mRNA level or the increased MTP mRNA level (22, 32). Other transcription factors may also play a role in these effects, such

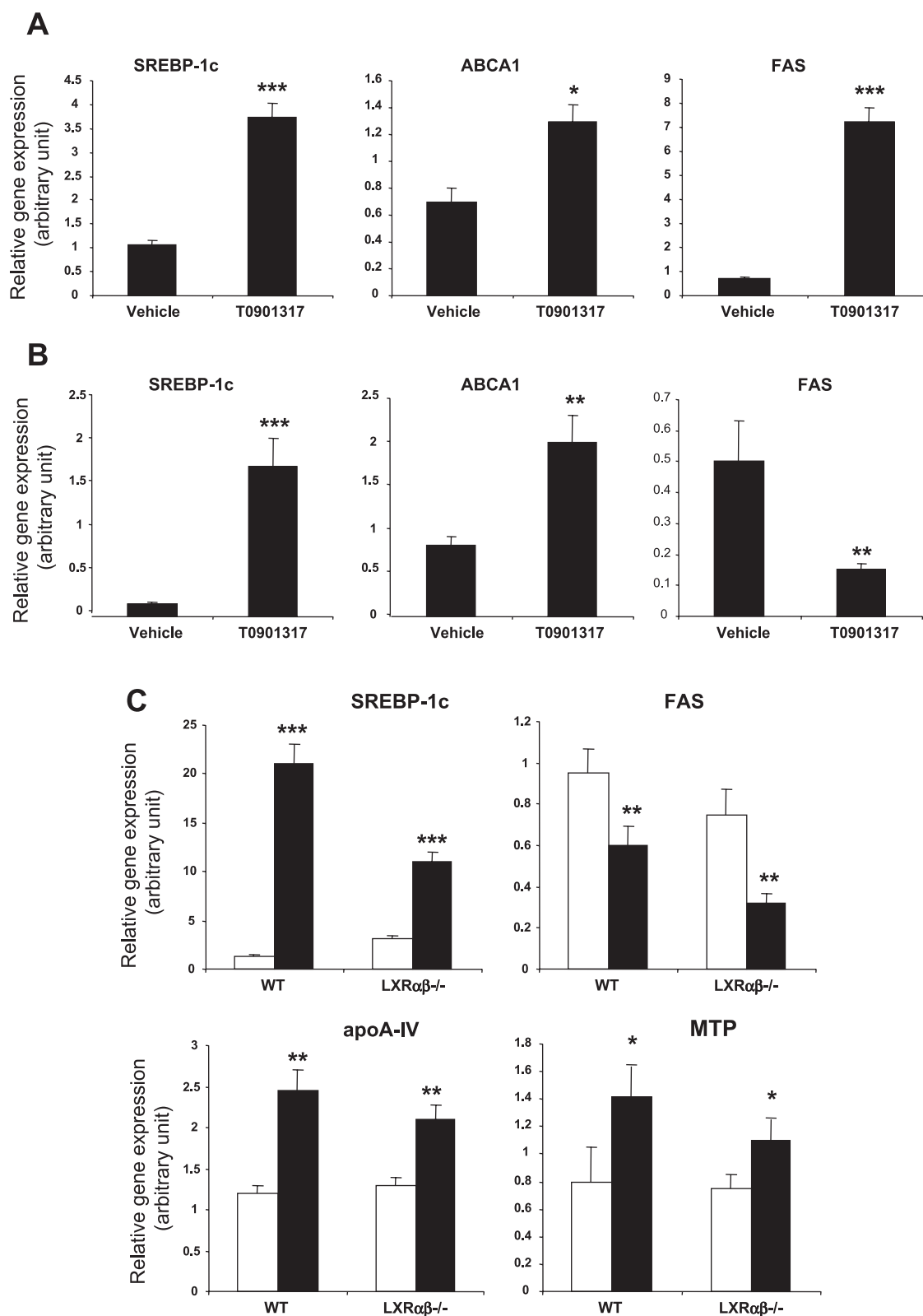


Fig. 8. Liver X receptor (LXR) and SREBP-1c activation after 7 days of HFD. After oral administration of LXR agonist T0901317 for 2 days, relative gene expressions were quantified by real-time PCR in liver (A) and intestine (B). C: relative intestinal gene expressions in LXR $\alpha\beta$ knockout mice and their wild-type littermates fed CD (open bars) or HFD (solid bars) for 7 days. Values were normalized to the 18S rRNA and expressed in arbitrary units; $n = 5$ for each condition. * $P < 0.05$; ** $P < 0.01$; *** $P < 0.001$ vs. CD.

as Sp1, NFY, or USF, which have been shown to bind to the proximal promoter of FAS and to control its transcription in response to dietary fatty acids in hepatocytes (9, 35), or HNF4, which is known to enhance the promoter activity of MTP gene (16). Further studies will clarify the mechanisms underlying the coordinated control of intestinal gene transcription during short-term HFD, a process that obviously involves complex interactions between transcription factors and coactivators or coinhibitors.

We report here that 7 days of HFD are sufficient to increase glycemia and insulinemia and to induce hepatic but not intestinal insulin resistance. Because it is known that insulin activates the transcription and the proteolytic maturation of SREBP-1c in several cell types (14), we suggest that activation of SREBP-1c in intestine may have resulted from the increased insulinemia, associated with a maintained sensitivity of intestine to insulin. Moreover, the decreased intestinal apoB48-TRL secretion could be related to the hyperinsulinemia and the intestinal insulin sensitivity. It was recently reported that a bolus of insulin induced a downregulation of apoB48-lipoprotein production in chow-fed hamsters. By contrast, during insulin-resistant state, intestine was not responsive to the inhibitory effect of insulin (7). However, in animal models and in humans, several studies have shown that diabetes or insulin resistance is associated with postprandial hypertriglyceridemia and with an increased secretion of apoB48-containing intestinal lipoproteins (5, 13, 28). Again, short-term HFD seems to be a particular period that could represent a transient state during which intestine is still sensitive to insulin and produces large chylomicrons whereas liver is already resistant to insulin but secretes less apoB100-containing lipoproteins. The physiological consequences of this short-term adaptation of intestinal lipid metabolism to HFD have to be evaluated. Indeed, it must be determined whether these changes represent the contribution of intestine to detrimental mechanisms that promote metabolic diseases and atherosclerosis or a beneficial adaptation that counteracts the lipid toxicity of high-fat diets.

In conclusion, the present study highlights the role that intestine plays, very early, in the adaptation to the fat content of the diet as well as in the control of postprandial triglyceridemia and questions the potential long-term consequences on metabolic diseases.

ACKNOWLEDGMENTS

The authors gratefully acknowledge Dr. D. J. Mangelsdorf (Howard Hughes Medical Institute, Dallas, TX) for providing LXR α / β knockout mice. We thank Luc Cynober for permitting triglyceride and cholesterol measurements in the biochemistry laboratory of Hôtel-Dieu hospital, Paris. We are grateful to Jean-Jacques Tousaint, Julie Biscan, and Maryse Séau for technical assistance.

GRANTS

S. J. Hernández Vallejo was the recipient of a grant from Laboratoires Pierre Fabre.

REFERENCES

1. Ayala J, Bracy D, McGuinness O, Wasserman D. Considerations in the design of hyperinsulinemic-euglycemic clamps in the conscious mouse. *Diabetes* 55: 390–397, 2006.
2. Botham K, Avella M, Cantafora A, Bravo E. The lipolysis of chylomicrons derived from different dietary fats by lipoprotein lipase in vitro. *Biochim Biophys Acta* 1349: 257–263, 1997.
3. Cartwright I, Higgins J. Increased dietary triacylglycerol markedly enhances the ability of isolated rabbit enterocytes to secrete chylomicrons: an effect related to dietary fatty acid composition. *J Lipid Res* 40: 1858–1866, 1999.
4. Cummins C, Volle D, Zhang Y, McDonald J, Sion B, Lefrançois-Martinez A, Caira F, Veysièrre G, Mangelsdorf D, Lobaccaro J. Liver X receptors regulate adrenal cholesterol balance. *J Clin Invest* 116: 1902–1912, 2006.
5. Duez H, Lamarche B, Uffelman K, Valero R, Cohn J, Lewis G. Hyperinsulinemia is associated with increased production rate of intestinal apolipoprotein B-48-containing lipoproteins in humans. *Arterioscler Thromb Vasc Biol* 26: 1357–1363, 2006.
6. Dugué-Pujol S, Rousset X, Pastier D, Quang N, Pautre V, Chambaz J, Chabert M, Kalopissis A. Human apolipoprotein A-II associates with triglyceride-rich lipoproteins in plasma and impairs their catabolism. *J Lipid Res* 47: 2631–2639, 2006.
7. Federico L, Naples M, Taylor D, Adeli K. Intestinal insulin resistance and aberrant production of apolipoprotein B48 lipoproteins in an animal model of insulin resistance and metabolic dyslipidemia: evidence for activation of protein tyrosine phosphatase-1B, extracellular signal-related kinase, and sterol regulatory element-binding protein-1c in the fructose-fed hamster intestine. *Diabetes* 55: 1316–1326, 2006.
8. Feedback on WHO/FAO global report on diet, nutrition, and non-communicable diseases. *Public Health Nutr* 6: 423–429, 2003.
9. Fukuda H, Noguchi T, Iritani N. Transcriptional regulation of fatty acid synthase gene and ATP citrate-lyase gene by Sp1 and Sp3 in rat hepatocytes(1). *FEBS Lett* 464: 113–117, 1999.
10. Gleeson A, Anderton K, Owens D, Bennett A, Collins P, Johnson A, White D, Tomkin G. The role of microsomal triglyceride transfer protein and dietary cholesterol in chylomicron production in diabetes. *Diabetologia* 42: 944–948, 1999.
11. Groot P, van Stiphout W, Krauss X, Jansen H, van Tol A, van Ramshorst E, Chin-On S, Hofman A, Cresswell S, Havekes L. Postprandial lipoprotein metabolism in normolipidemic men with and without coronary artery disease. *Arterioscler Thromb* 11: 653–662, 1991.
12. Grønholdt M, Nordestgaard B, Nielsen T, Sillesen H. Echolucent carotid artery plaques are associated with elevated levels of fasting and postprandial triglyceride-rich lipoproteins. *Stroke* 27: 2166–2172, 1996.
13. Haidari M, Leung N, Mahhub F, Uffelman K, Kohen-Avramoglu R, Lewis G, Adeli K. Fasting and postprandial overproduction of intestinally derived lipoproteins in an animal model of insulin resistance. Evidence that chronic fructose feeding in the hamster is accompanied by enhanced intestinal de novo lipogenesis and ApoB48-containing lipoprotein overproduction. *J Biol Chem* 277: 31646–31655, 2002.
14. Hegarty B, Bobard A, Hainault I, Ferré P, Bossard P, Foufelle F. Distinct roles of insulin and liver X receptor in the induction and cleavage of sterol regulatory element-binding protein-1c. *Proc Natl Acad Sci USA* 102: 791–796, 2005.
15. Humber J, Missano B, Rudling M, Hennes U, Kempen H. Effects of stigmastanyl-phosphocholine (Ro 16–6532) and lovastatin on lipid and lipoprotein levels and lipoprotein metabolism in the hamster on different diets. *J Lipid Res* 36: 1567–1585, 1995.
16. Hirokane H, Nakahara M, Tachibana S, Shimizu M, Sato R. Bile acid reduces the secretion of very low density lipoprotein by repressing microsomal triglyceride transfer protein gene expression mediated by hepatocyte nuclear factor-4. *J Biol Chem* 279: 45685–45692, 2004.
17. Hussain M. A proposed model for the assembly of chylomicrons. *Atherosclerosis* 148: 1–15, 2000.
18. Kalopissis A, Griglio S, Le Liepvre X. Intestinal very low density lipoprotein secretion in rats fed various amounts of fat. *Biochim Biophys Acta* 711: 33–39, 1982.
19. Karpe F, Steiner G, Uffelman K, Olivecrona T, Hamsten A. Postprandial lipoproteins and progression of coronary atherosclerosis. *Atherosclerosis* 106: 83–97, 1994.
20. Kawano K, Qin S, Vieu C, Collet X, Jiang X. Role of hepatic lipase and scavenger receptor BI in clearing phospholipid/free cholesterol-rich lipoproteins in PLTP-deficient mice. *Biochim Biophys Acta* 1583: 133–140, 2002.
21. Kim J, Gimeno R, Higashimori T, Kim H, Choi H, Punreddy S, Mozell R, Tan G, Stricker-Krongrad A, Hirsch D, Fillmore J, Liu Z, Dong J, Cline G, Stahl A, Lodish H, Shulman G. Inactivation of fatty acid transport protein 1 prevents fat-induced insulin resistance in skeletal muscle. *J Clin Invest* 113: 756–763, 2004.

22. **Latasa M, Griffin M, Moon Y, Kang C, Sul H.** Occupancy and function of the -150 sterol regulatory element and -65 E-box in nutritional regulation of the fatty acid synthase gene in living animals. *Mol Cell Biol* 23: 5896–5907, 2003.
23. **Lewis G, Uffelman K, Naples M, Szeto L, Haidari M, Adeli K.** Intestinal lipoprotein overproduction, a newly recognized component of insulin resistance, is ameliorated by the insulin sensitizer rosiglitazone: studies in the fructose-fed Syrian golden hamster. *Endocrinology* 146: 247–255, 2005.
24. **Mu H, Høy C.** Intestinal absorption of specific structured triacylglycerols. *J Lipid Res* 42: 792–798, 2001.
25. **Oliveros L, Videla A, Ramirez D, Gimenez M.** Dietary fat saturation produces lipid modifications in peritoneal macrophages of mouse. *J Nutr Biochem* 14: 370–377, 2003.
26. **Patsch J, Miesenböck G, Hopferwieser T, Mühlberger V, Knapp E, Dunn J, Gotto AJ, Patsch W.** Relation of triglyceride metabolism and coronary artery disease. Studies in the postprandial state. *Arterioscler Thromb* 12: 1336–1345, 1992.
27. **Phillips C, Bennett A, Anderton K, Owens D, Collins P, White D, Tomkin G.** Intestinal rather than hepatic microsomal triglyceride transfer protein as a cause of postprandial dyslipidemia in diabetes. *Metabolism* 51: 847–852, 2002.
28. **Phillips C, Murugasu G, Owens D, Collins P, Johnson A, Tomkin G.** Improved metabolic control reduces the number of postprandial apolipoprotein B-48-containing particles in type 2 diabetes. *Atherosclerosis* 148: 283–291, 2000.
29. **Phillips M, Pullinger C, Kroes I, Kroes J, Hardman D, Chen G, Curtiss L, Gutierrez M, Kane J, Schumaker V.** A single copy of apolipoprotein B-48 is present on the human chylomicron remnant. *J Lipid Res* 38: 1170–1177, 1997.
30. **Pruneta V, Autran D, Ponsin G, Marçais C, Duvillard L, Verges B, Berthezene F, Moulin P.** Ex vivo measurement of lipoprotein lipase-dependent very low density lipoprotein (VLDL)-triglyceride hydrolysis in human VLDL: an alternative to the postheparin assay of lipoprotein lipase activity? *J Clin Endocrinol Metab* 86: 797–803, 2001.
31. **Redgrave T.** Chylomicron metabolism. *Biochem Soc Trans* 32: 79–82, 2004.
32. **Sato R, Miyamoto W, Inoue J, Terada T, Imanaka T, Maeda M.** Sterol regulatory element-binding protein negatively regulates microsomal triglyceride transfer protein gene transcription. *J Biol Chem* 274: 24714–24720, 1999.
33. **Stewart-Phillips J, Lough J, Skamene E.** Genetically determined susceptibility and resistance to diet-induced atherosclerosis in inbred strains of mice. *J Lab Clin Med* 112: 36–42, 1988.
34. **Taghibiglou C, Carpentier A, Van Iderstine S, Chen B, Rudy D, Aiton A, Lewis G, Adeli K.** Mechanisms of hepatic very low density lipoprotein overproduction in insulin resistance. Evidence for enhanced lipoprotein assembly, reduced intracellular ApoB degradation, and increased microsomal triglyceride transfer protein in a fructose-fed hamster model. *J Biol Chem* 275: 8416–8425, 2000.
35. **Teran-Garcia M, Rufo C, Nakamura M, Osborne T, Clarke S.** NF- κ B involvement in the polyunsaturated fat inhibition of fatty acid synthase gene transcription. *Biochem Biophys Res Commun* 290: 1295–1299, 2002.
36. **Tholstrup T, Ehnholm C, Jauhiainen M, Petersen M, Høy C, Lund P, Sandström B.** Effects of medium-chain fatty acids and oleic acid on blood lipids, lipoproteins, glucose, insulin, and lipid transfer protein activities. *Am J Clin Nutr* 79: 564–569, 2004.
37. **Tornvall P, Olivecrona G, Karpe F, Hamsten A, Olivecrona T.** Lipoprotein lipase mass and activity in plasma and their increase after heparin are separate parameters with different relations to plasma lipoproteins. *Arterioscler Thromb Vasc Biol* 15: 1086–1093, 1995.
38. **Van Heek M, Zilversmit D.** Postprandial lipemia and lipoprotein lipase in the rabbit are modified by olive and coconut oil. *Arteriosclerosis* 10: 421–429, 1990.
39. **Vidal R, Hernandez-Vallejo S, Pauquai T, Texier O, Rousset M, Chambaz J, Demignot S, Lacorte J.** Apple procyanidins decrease cholesterol esterification and lipoprotein secretion in Caco-2/TC7 enterocytes. *J Lipid Res* 46: 258–268, 2005.
40. **Weintraub M, Zechner R, Brown A, Eisenberg S, Breslow J.** Dietary polyunsaturated fats of the W-6 and W-3 series reduce postprandial lipoprotein levels. Chronic and acute effects of fat saturation on postprandial lipoprotein metabolism. *J Clin Invest* 82: 1884–1893, 1988.
41. **Xiang S, Cianflone K, Kalant D, Sniderman A.** Differential binding of triglyceride-rich lipoproteins to lipoprotein lipase. *J Lipid Res* 40: 1655–1663, 1999.